Inhibition of cytosolic translation mitigates mitochondrial dysfunction in *C. elegans*

Avijit Mallick, Yunguang Du, Theresa Ramalho, Rui Li, Levi Ali, Sookyung Kim, Lihua Julie Zhu, and Cole M. Haynes

Department of Molecular, Cell, and Cancer Biology,

University of Massachusetts Chan Medical School, Worcester, MA 01605, USA.

Abstract

The mitochondrial unfolded protein response (UPR^{mt}) is regulated by the bZIP protein ATFS-1 which promotes mitochondrial protein homeostasis (proteostasis) and mitochondrial biogenesis in *Caenorhabditis elegans*. Upon mitochondrial perturbation, the ATFS-1-dependent transcriptional program promotes gene expression, leading to mitochondrial recovery. Conversely, *atfs-1*-deletion worms harbor dysfunctional mitochondria, are developmentally impaired, and short-lived. However, *atfs-1*-deletion worms develop to adults suggesting the presence of other signaling pathways that promote mitochondrial function and biogenesis in the absence of *atfs-1*. We hypothesized that additional transcription factors regulate, or promote, mitochondrial function in the absence of *atfs-1*. Here, we screened for transcription factors that could reduce the decline in mitochondrial function in the atfs-1 mutants when inhibited. Here, we demonstrate that inhibition of the nuclear hormone receptor NHR-180 re-establishes a functional mitochondrial network in *atfs-1(null)* worms, increases mtDNA content, and improves the developmental rate of wildtype worms. NHR-180 increases transcription of genes required for cytosolic protein synthesis in response to mitochondrial perturbation. Inhibition of the S6 kinase homolog, *rsks-1*, in *atfs-1(null)* worms leads to a recovery of the mitochondrial network and mtDNA content consistent with *nhr-180* regulating expression of protein synthesis components. Consistent with the observations in *C. elegans*, S6 kinase inhibition also increased mitochondrial biogenesis in mammalian *atf5*-knockout cells that harbor severely impaired mitochondria. Intriguingly, *nhr-180* or S6 kinase inhibition also rescues mitochondrial dysfunction caused by mutations in multiple genes required for oxidative phosphorylation. Combined, these studies suggest that increased protein synthesis contributes to the mitochondrial dysfunction caused by perturbations in OXPHOS gene expression and suggest a relatively straightforward approach to reducing the impact of mitochondrial dysfunction.

Keywords: NHR-180, ATFS-1, mitochondria, OXPHOS, mtDNA, protein synthesis

Introduction

Mitochondria are membrane-bound organelles dispersed throughout the cytosol of eukaryotic cells. They are required for essential cellular processes including ATP production, lipid oxidation, nucleotide and amino acid synthesis, and regulating programmed cell death and innate immune signaling (1–3). Mitochondrial dysfunction is linked to various debilitating diseases including Parkinson's and Alzheimer's Disease (4, 5). This specialized organelle comprises proteins mostly encoded by the nuclear genome; however, the mitochondrial genome (mtDNA) encodes essential OXPHOS proteins (12 in *Caenorhabditis elegans*; 13 in mammals). The mitochondrial-localized encoded by nuclear genes are translated on cytosolic ribosomes. Most mitochondrial-localized proteins harbor a mitochondrial-targeting sequence required for import into mitochondria via import channels localized in the mitochondrial outer membrane as well as in the inner membrane.

The mitochondrial unfolded protein response (UPR^{mt}) is a mitochondria-to-nuclear signaling pathway mediated by the bZIP protein ATFS-1 which promotes mitochondrial protein quality control, mitochondrial biogenesis and expansion during cell growth (6). When the mitochondria population is healthy, most of the ATFS-1 is efficiently imported into mitochondria where it is degraded by the protease LONP-1 (1, 2, 7). In contrast, upon mitochondrial perturbations such as OXPHOS dysfunction, or impaired mitochondrial proteostasis, ATFS-1 fails to be imported into mitochondrial and translocate to the nucleus to induce the UPR^{mt} which promotes recovery of mitochondrial function, longevity, and resistance to infection, (8–10). Importantly, *atfs*-1-deletion causes dysfunctional mitochondria, reduction in mtDNAs, impaired development, reduced lifespan (8, 11, 12).

While mitochondrial function is compromised in *atfs-1(null)* worms, they develop into mature adults, albeit at a slower rate than wildtype worms. In this study, we questioned whether additional transcription factors are activated during mitochondrial dysfunction in the absence of *atfs-1*. We identified and tested multiple transcription factors that were differentially expressed in the *atfs-1(null)* mutants. We reasoned that transcription factors that are expressed significantly differently in the *atfs-1* mutants may contribute to the mitochondrial function, or dysfunction in the *atfs-1(null)* worms. We then inhibited the expression of each transcription factor in *atfs-1(null)* worms and compared the growth rate to wildtype and *atfs-1*(null) worms. To our surprise, inhibition of 5 of the 76 tested transcription factors accelerated growth in *atfs-1(null)* worms. We identified five transcription factors (*ceh-49*, *lsl-1*, *nhr-2*, *nhr-180,* and *tbx-9*)

that suppressed the growth delay when inhibited in *atfs-1(null)* worms. From this narrowed-down list, *nhr-180* was the only downregulated TF in the *atfs-1* mutants. Intriguingly, inhibition of *nhr-180* expression also rescued the developmental delay in worms harboring hypomorphic mutations in essential OXPHOS genes (*isp-1(qm30*), *clk-1(qm150)*.

Here we demonstrate that the previously uncharacterized transcription factor *nhr-180* regulates mitochondrial function. Remarkably, in addition to rescuing the slow growth in worms with dysfunctional mitochondria, the inhibition of NHR-180 increased mtDNA, and improved mitochondrial function in *atfs-1(null)* as well as in worms with mutations in OXPHOS genes. We propose a model in which increased *nhr-180*-dependent transcription enhances the expression of genes encoding translation machinery in both the cytosol and mitochondria during mitochondrial dysfunction. However, as reduced *nhr-180* activity promotes mitochondrial function in *atfs-1(null)* worms and OXPHOS mutants, we propose that the increased protein synthesis associated with NHR-180 activity contributes additional proteostasis stress to the mitochondrial network in *atfs-1(null), clk-1(qm150)*, *isp-1(qm30)* worms. Consistent with the model, we demonstrate that reduced expression of the S6 kinase homolog *rsks-1*, or activation of the AMPK homolog *aak-2*, which both reduce protein synthesis, also promotes mitochondrial recovery in *atfs-1(null*) worms and the OXPHOS mutants. Combined, our findings suggest a novel approach and targets to recover mitochondrial dysfunction in disease as well during aging.

Results

Identification of transcription factors that impact mitochondrial function

The bZIP transcription factor ATFS-1 is required to activate the UPR^{mt} in *C. elegans* ((1, 7, 9, 12, 13). Worms lacking *atfs-1* have severe mitochondria dysfunction, abnormal mitochondria morphology, reduced mtDNA content, increased susceptibility to oxidative stress and infection, and a developmental delay (9–11). However, while delayed, worms lacking ATFS-1 develop into mature adults. Here, we sought to identify additional transcription factors that impact mitochondrial function and development in the absence of ATFS-1.

We first identified transcription factors that are differentially expressed in *atfs-1(null)* worms using our previously published RNAseq data (6), where we compared the transcriptomes of wildtype and *atfs-1(null)* worms (Fig. 1A). We identified 76 genes differentially

expressed *atfs-1(null)* worms relative to wildtype worms and subsequently knocked down each of the 76 genes in *atfs-1(null)* worms and examined the impact on the rate of development. Ten genes were identified that altered the development rate of *atfs-1(null)* worms. Inhibition of *nhr-2, tbx-9, lsl-1, ceh-49,* or *nhr-180* increased the developmental rate of *atfs-1(null)* worms (Fig. 1B and C). Interestingly, *nhr-180* mRNA was reduced in *atfs-1(null)* worms relative to wildtype worms, *nhr-2, tbx-9, lsl-1* and *ceh-49* mRNAs were increased in *atfs-1(null)* worms relative to wildtype worms. Of these, inhibition of *nhr-2* and *nhr-180* increased the rate of *atfs-1(null)* worm development the most, which was comparable to wildtype animals (Fig. 1B and C).

Next, we determined the effect of *nhr-2* or *nhr-180* inhibition on the growth rate of other mitochondrial mutants such as the well-characterized OXPHOS mutant alleles *clk-1(qm30)*, which is defective in ubiquinone biosynthesis and *isp-1(qm150),* which has an impaired component of OXPHOS complex III with reduced OXPHOS activity (cytochrome c oxidoreductase). Interestingly, reduced expression of *nhr-2* or *nhr-180* increased the developmental rate of both OXPHOS mutant strains (Fig. 1D-G). As *nhr-180*(RNAi) caused the stronger growth phenotype, we have focused the remainder of our studies on NHR-180.

To determine the impact of *nhr-180* inhibition on mitochondrial function, we stained mitochondria with the dye TMRE (Tetramethyl rhodamine, Ethyl Ester, Perchlorate) which accumulates within functional mitochondria due to the OXPHOS-mediated inner membrane potential (11, 14). As expected, TMRE staining is reduced in *atfs-1(null)* worms relative to wildtype worms. However, TMRE staining is increased in *atfs-1(null)* worms when *nhr-180* is knocked by RNAi to levels comparable to wildtype worms (Fig. 1H). Consistent with increased inner mitochondrial membrane potential, *nhr-180*(RNAi) also increased the lifespan and mitochondrial DNA (mtDNA) content in *atfs-1(null)* worms (Fig. 1I-K). Combined, these data suggest that *nhr-180* inhibition partially increases mitochondrial function and genome in worms lacking *atfs-1*. Furthermore, these findings suggest that *nhr-180*-dependent transcription contributes to the mitochondrial dysfunction observed in *atfs-1(null)* and *isp-1(qm150)* worms.

nhr-180 **deletion increases mitochondrial function in** ***atfs-1*** **mutants**

We next sought to determine if the increased mitochondrial function observed in the OXPHOS mutant worms is caused by a partial loss of NHR-180 function caused by RNAi. Via

CRISPR-Cas9 mediated genome editing, we introduced 4 stop codons into the first exon of the *nhr-180* gene which was confirmed by sequencing and the lack of *nhr-180* mRNA expression (Fig 2A). Surprisingly, *nhr-180(cmh19)* worms have a shorter lifespan at both 20°C and 25°C compared to wildtype worms (Fig. 2B and C). However, *atfs-1(null);nhr-180(cmh19)* had a significantly increased lifespan relative to *atfs-1(null)* worms (Fig. 2D). Importantly, *atfs-1(null);nhr-180(cmh19)* also exhibited increased body bending/thrashing rate compared to *atfs-1(null)* worms. Similar to the phenotypes observed when worms are raised on *nhr-180*(RNAi), *atfs-1(null);nhr-180(cmh19)* worms exhibit increased TMRE staining and increased mtDNA content compared to *atfs-1(null)* worms consistent with a more robust mitochondrial network (Fig. 2E-G). Combined, these findings suggest that the improved fitness of *atfs-1(null)* worms caused by impaired NHR-180 expression is due to increased mitochondrial function.

Mitochondrial function declines as worms age (15). However, we found that at adult day-4, *nhr-180(cmh19)* worms have significantly more TMRE staining relative to wildtype worms (Fig. 2H). While *nhr-180* mutants have lower brood size compared to wildtype worms, *atfs-1(null);nhr-180(cmh19)* worms laid more eggs than *atfs-1(null)* worms (Fig. 2I). Because ATFS-1-dependent UPR^{mt} activation shows increased oxidative stress and infection resistance (9, 16, 17), we examined *nhr-180* mutant phenotypes under these conditions. Consistent with their reduced lifespan, *nhr-180* mutants show increased susceptibility to paraquat treatment but similar survivability on *P. aeruginosa* (Fig. 2J and K).

Combined, our data suggest that impaired expression of NHR-180 promotes mitochondrial function in worms with severe mitochondrial dysfunction including *atfs-1*-deletion worms as well worms with mutations in essential OXPHOS components.

NHR-180 expression occurs in the intestine, hypodermis, and muscle

To gain insight into the expression pattern of NHR-180, we generated a translational reporter where NHR-180 was tagged with GFP at the C-terminus (*nhr-180*$_{pr}$*::nhr-180::GFP*) (Fig. 3A). We found that NHR-180 is expressed in eggs and continues throughout development into adulthood. While NHR-180::GFP expression is most obvious in the intestine, NHR-180::GFP is also expressed in muscle cells and the hypodermis (Fig. 3B). Within the intestinal cells, NHR-180::GFP is located in both the cytosol and nucleus. However, in muscle and

hypodermal cells NHR-180::GFP is only in the nucleus (Fig. 3B). To confirm that the GFP expression correlates with the levels of NHR-180, we observe a complete abolishment of GFP following *nhr-180*(RNAi) (Fig 3D).

We next sought to determine the physiologic conditions that induce *nhr-180* expression. We exposed *nhr-180*$_{pr}$::*nhr-180*::gfp expressing worms to paraquat (oxidative stress), *P. aeruginosa* (infection), or tunicamycin (ER stress). Only paraquat treatment increased the intensity of NHR-180-GFP as well as its nuclear localization (Fig. 3C). However, an accumulation of NHR-180-GFP is also seen in the cytosolic compartment. Additionally, we have confirmed this increase in *nhr-180* expression following paraquat treatment by qPCR in N2 animals (Fig. 3E). These findings are consistent with previously published transcriptomic data showing that *nhr-180* transcripts are induced upon exposure to paraquat in wildtype worms, but also induced OXPHOS mutants such as *isp-1(qm150)*, *clk-1(qm30)*, and *nuo-6(qm200)* (16, 18). All of the mutations in the OXPHOS components *isp-1(qm150)*, *clk-1(qm30), nuo-6(qm200)* result in increased *atfs-1*-dependent transcription activation which in turn leads to increased *nhr-180* transcription (Fig. 3F). Combined, these data suggest that during mitochondrial perturbation, *nhr-180* expression is elevated to promote mitochondrial biogenesis.

Transcription of genes required for cytosolic and mitochondrial protein synthesis is repressed in the *nhr-180*-deletion worms

To gain insight into the role of NHR-180, we carried out transcriptomic analysis in wildtype, *nhr-180(cmh19)*, *atfs-1(null)*, and *atfs-1(null); nhr-180(cmh19)* at the L4 stage. We found that ~1380 genes are upregulated in *nhr-180(cmh19)* worms and ~750 genes are downregulated compared to wildtype worms (Fig. 4A and B, Supplementary Table 1). Interestingly, gene enrichment analyses indicate that genes required for cytosolic protein synthesis and protein synthesis within mitochondria are significantly reduced in *nhr-180(cmh19)* worms (Fig. 4C and D). Combined, these findings suggest a role for NHR-180 in promoting mitochondrial biogenesis, perhaps in conjunction with ATFS-1.

Intriguingly, *nhr-180* mutants reverse the expression of genes seen in *atfs-1(null)* worms (Fig. 4E). Intriguingly, genes that are upregulated in the *atfs-1(null);nhr-180(cmh19)* worms compared to *atfs-1(null)* worms are involved in promoting dauer metabolism and larval

development (Supplementary Table 2). Additionally, *nhr-180* mutant worms increase the transcription of genes that are downregulated in the OXPHOS mutants (Fig. 4F, Supplementary Table 3) (19). In both *atfs-1* and OXPHOS mutants, inhibition of *nhr-180* enhances the expression of genes involved in dauer metabolism and larval development which supports our findings of increased growth rate seen in OXPHOS mutants after *nhr-180* knockdown.

We next compared gene expression in *nhr-180* mutant worms with dietarily restricted worms as this condition represses anabolism and promotes catabolism to promote survival during reduced nutrition. *eat-2* mutant worms are a dietary restriction model in worms as they have a reduced rate of food consumption (20). Surprisingly, 554 of the upregulated genes in *nhr-180* mutants are also upregulated in the *eat-2* mutants (Fig. 5A, Supplementary Table 4) (21). The benefits linked to dietary restriction require AMPK activation and the downstream phosphorylation of S6 kinase which leads to reduced protein synthesis (22, 23). To further examine the impact of protein synthesis we examined the impact of decreasing the rate of protein synthesis by using a strain that expresses the constitutively active allele of AMPK CA-AAK-2 which leads to similar phenotypes to those observed during dietary restriction (24). Genes upregulated in *nhr-180* mutants significantly overlaps with those in the CA-AAK-2 mutant (Supplementary Table 5). However, *nhr-180* expression is not affected in *aak-2* or *rsks-1* mutant worms (25, 26). Combined, our data suggest that *nhr-180* regulates a transcriptional program that promotes protein synthesis in both the mitochondrial matrix and on cytosolic ribosomes, which is induced during mitochondrial dysfunction.

RSKS-1 inhibition rescues mitochondrial dysfunction

We next examined if the constitutively active form of the catalytic AMPK subunit AAK-2 (CA-AAK-2) or deletion of the S6 kinase homolog RSKS-1, both of which reduce protein synthesis, affected mitochondrial function and the development of *atfs-1(null)* worms (23, 27). Impressively, expression of CA-AAK-2 or inhibition of *rsks-1* expression increased TMRE staining in *atfs-1(null)* worms to a level similarly to that observed in wildtype worms (Fig. 5B and C). Importantly, the lifespan of *atfs-1(null)* worms also increased significantly (Fig. 5D and E). As an alternative approach to evaluating mitochondrial biogenesis and function, we determined the mtDNA content in the *atfs-1(null)* worms when raised on *rsks-1*(RNAi).

Consistent with the increased mitochondrial function of *atfs-1(null)* worms raised on *rsks-1*(RNAi) (Fig 5B and C), mtDNA content was also increased (Fig. 5F).

To investigate further, we questioned whether starvation can also lead to a similar phenotype. To this end, we starved *atfs-1* mutants for 3 generations before analyzing their lifespan and health span (Fig. 5G). Phenotypes were examined after worms were recovered and fed on the bacterial diet. Surprisingly enough, starved *atfs-1(null)* mutants lived significantly longer compared to *atfs-1(null)* that were continuously fed (Fig. 5H). Moreover, starved *atfs-1(null)* mutants exhibited better TMRE staining, body bending, and thrashing rates (Supplementary Fig. 1C). However, such phenotypic differences were absent in intermittently starved versus un-starved wild-type animals (Fig. 5H). Such a rescue in the *atfs-1(null)* phenotypes was abolished when worms were refed for two successive generations suggesting a lack of permanent genetic modification in these mutants.

To determine if the impact of S6 kinase inhibition on mitochondrial function is conserved in mammals, via genome editing we generated HEK293T cells with impaired ATF5 expression, which is the mammalian homolog of ATFS-1 that regulates the UPR^{mt} in mammals (28). Similar to *atfs-1(null)* worms, ATF5-/- cells have reduced mtDNA content, and respire less as determined by Seahorse (11, 28). Interestingly, treatment with the S6 kinase inhibitor (PF-4708671) increased mtDNA content in the absence of ATF5, suggesting that the regulation of mitochondrial function by S6 kinase is conserved (Fig. 5I) (29). Furthermore, S6 kinase inhibition increased mtDNA content is seen in the wild-type cells only at the high dose of 100μm (Fig. 5I). Combined, these data suggest that a reduction in cytosolic protein synthesis in mammalian cells improves mitochondrial function similarly to that observed in *C. elegans*.

Discussion

The UPR^{mt} was discovered as a pathway that responds to mitochondrial perturbations including the accumulation of unfolded proteins in mitochondria as well as impaired expression of OXPHOS components. In response to mitochondrial dysfunction, *atfs-1*-dependent transcription is increased which includes genes that promote mitochondrial proteostasis and mitochondrial biogenesis. UPR^{mt} activation also promotes resistance to pathogen infection and increased longevity (9, 17, 30). However, most of the mitochondrial mutants, including OXPHOS mutants show slower larval development (16, 18). Here, we propose a model

whereby cells respond to mild mitochondrial dysfunction by activating a cytosolic response via *nhr-180*, promoting both cytosolic and mitochondrial translation and suppressing genes required for larval development. This *nhr-180*-mediated transcriptional response promotes mitochondrial biogenesis and slows down larval development. However, mitochondrial dysfunction caused by genetic mutations such as *isp-1* and *clk-1* leads to constitutive activation of *nhr-180*. In line with our model, we propose that elevated cytosolic and mitochondrial protein synthesis during mitochondrial dysfunction caused by mutations further aggravates the mitochondrial condition. Encouraging mitochondrial biogenesis by *nhr-180* likely exacerbates the accumulation of mutated mitochondrial proteins, further impairing organelle function.

In this study, we show that mitochondrial defect leads to the induction of *nhr-180* which slows development and exacerbates phenotypes seen in the mitochondrial mutants by promoting cytosolic and mitochondrial protein synthesis. NHR-180 suppresses genes required for larval development and lipid breakdown but promotes genes involved in cytosolic and mitochondrial protein synthesis. This leads to a further decline in mitochondria function. We show that by reducing *nhr-180* expression or by mutating the gene, the mitochondrial function can be elevated in *atfs-1* mutant worms or those with OXPHOS defects. Similar attenuation of mitochondrial dysfunction is also seen following activation of AAK-2/AMPK or reducing RSKS-1/S6 kinase activity, where both conditions lead to reduced cytosolic protein synthesis. Collectively, these data suggest that reducing translation alleviates mitochondrial stress caused by excessive protein accumulation, misfolding, and aggregation under conditions of mitochondrial dysfunction.

Glucose is required for mitochondrial OXPHOS to generate energy demand for cells. However, too much glucose harms mitochondrial function due to excessive reactive oxygen species (ROS) generation inside mitochondria (31, 32). Intriguingly, research on *C. elegans* shows that impaired glucose metabolism leads to increased mitochondrial respiration and better lifespan (33). This effect of caloric requires AMPK (27, 34). Similarly, dietary restriction or activated AMPK delays age-associated decline in mitochondrial network and function in both worms and mice (24, 35). Our findings of recovery of mitochondrial defects via inhibition of protein translation are in line with the understanding of the beneficial effects of dietary restriction on mitochondrial function (24). Such a phenomenon appears to be conserved across eukaryotes (27, 35).

An unbiased screen in yeast cells previously identified 40 suppressors of mitochondrial dysfunction-induced cell death (36, 37). These suppressors included five classes of genes associated with the target of rapamycin (TOR) signaling, mRNA silencing and turnover, ribosomal function, protein translation, transfer RNA methylation, and cytosolic protein chaperoning and degradation (36). Another independent study analyzed all the RNA transcripts and proteins that are altered in cells in which mitochondrial import is impaired. Strikingly, expression and production of many of the genes and proteins required for protein synthesis were reduced, as was overall protein synthesis (38). Furthermore, mTOR inhibition that slows down growth and protein translation has been shown to mitigate mitochondrial dysfunction-associated phenotypes in mice (39). These independent findings align conceptually with the beneficial effects of inhibiting *nhr-180* observed in worms, where reduced cytosolic and mitochondrial protein synthesis alleviates declines in mitochondrial function.

In *nhr-180* mutants, mitochondrial protein transporters, mitochondrial translation elongation factors, mitochondrial ribosomal subunit, and cytosolic translation initiation factors are downregulated. Our study suggests a mechanism where dysfunctional mitochondria can be partially restored by reducing global protein translation. Inhibiting *nhr-180*, which suppresses mitochondrial biogenesis in defective mitochondrial mutants, leads to the remarkable recovery of mitochondrial function. Similarly, mitochondrial recovery can be achieved by inhibiting *rsks-1* or activating *aak-2*. Collectively, our findings demonstrate a straightforward yet effective strategy to ameliorate mitochondrial dysfunction in diseases linked to mutations in mitochondrial components.

Acknowledgments

We thank the *Caenorhabditis* Genetics Center for providing *C. elegans* strains (funded by NIH Office of Research 362 Infrastructure Programs (P40OD010440), and the UMass Medical School Core facilities for deep sequencing. This work was supported by the National Institutes of Health grants (R01AG040061 and R01AG047182) to C.M.H. and the Natural Sciences and Engineering Research Council (NSERC) postdoctoral fellowship to A.M. The authors are solely responsible for the content.

Author contributions

A.M. and C.M.H. planned the experiments. A.M. and Y.D. generated worm strains. A.M. performed RNA-seq, lifespan analysis, qPCR, and TMRE experiments. R.L., and L.J.Z. analyzed the sequencing data. L.A. and S.K. performed some of the experiments. T.R. performed mammalian cell culture assays. A.M. and C.M.H. wrote the manuscript.

Declaration of interests

The authors declare no competing interests.

References

1. T. Shpilka, C. M. Haynes, The mitochondrial UPR: Mechanisms, physiological functions and implications in ageing. *Nat. Rev. Mol. Cell Biol.* **19**, 109–120 (2018).

2. N. S. Anderson, C. M. Haynes, Folding the Mitochondrial UPR into the Integrated Stress Response. *Trends Cell Biol.* **30**, 428–439 (2020).

3. R. Higuchi-Sanabria, P. A. Frankino, J. W. Paul, S. U. Tronnes, A. Dillin, A Futile Battle? Protein Quality Control and the Stress of Aging. *Dev. Cell* **44**, 139–163 (2018).

4. W. Wang, F. Zhao, X. Ma, G. Perry, X. Zhu, Mitochondria dysfunction in the pathogenesis of Alzheimer's disease: Recent advances. *Mol. Neurodegener.* **15**, 1–22 (2020).

5. G. B. Irvine, O. M. El-Agnaf, G. M. Shankar, D. M. Walsh, Protein aggregation in the brain: The molecular basis for Alzheimer's and Parkinson's diseases. *Mol. Med.* **14**, 451–464 (2008).

6. T. Shpilka, *et al.*, UPRmt scales mitochondrial network expansion with protein synthesis via mitochondrial import in Caenorhabditis elegans. *Nat. Commun.* **12** (2021).

7. A. Nargund, M. W. Pellegrino, C. J. Fiorese, B. M. Baker, C. M. Haynes, Mitochondrial Import Efficiency of ATFS-1 Regulates Mitochondrial UPR Activation. *Science (80-.).* **337**, 587–590 (2012).

8. N. Uma Naresh, *et al.*, Mitochondrial genome recovery by ATFS-1 is essential for development after starvation. *Cell Rep.* **41**, 111875 (2022).

9. M. W. Pellegrino, *et al.*, Mitochondrial UPR-regulated innate immunity provides resistance to pathogen infection. *Nature* **516**, 414–417 (2014).

10. Z. Wu, *et al.*, Mitochondrial unfolded protein response transcription factor ATFS-1 promotes longevity in a long-lived mitochondrial mutant through activation of stress response pathways. *BMC Biol.* **16**, 1–19 (2018).

11. Q. Yang, *et al.*, LONP-1 and ATFS-1 sustain deleterious heteroplasmy by promoting mtDNA replication in dysfunctional mitochondria. *Nat. Cell Biol.* **24**, 181–193 (2022).

12. Y. F. Lin, *et al.*, Maintenance and propagation of a deleterious mitochondrial genome by the mitochondrial unfolded protein response. *Nature* **533**, 416–419 (2016).

13. A. M. Nargund, C. J. Fiorese, M. W. Pellegrino, P. Deng, C. M. Haynes, Mitochondrial and nuclear accumulation of the transcription factor ATFS-1 promotes OXPHOS recovery during the UPRmt. *Mol. Cell* **58**, 123–133 (2015).

14. A. Mallick, C. M. Haynes, Methods to analyze the mitochondrial unfolded protein response (UPRmt). *Methods Enzymol.* **707**, 543–564 (2024).

15. C. J. Gaffney, *et al.*, Greater loss of mitochondrial function with ageing is associated with earlier onset of sarcopenia in C. elegans. *Aging (Albany. NY).* **10**, 3382–3396 (2018).

16. W. Yang, S. Hekimi, A mitochondrial superoxide signal triggers increased longevity in caenorhabditis elegans. *PLoS Biol.* **8** (2010).

17. P. Deng, *et al.*, Mitochondrial UPR repression during Pseudomonas aeruginosa infection

requires the bZIP protein ZIP-3. *Proc. Natl. Acad. Sci. U. S. A.* **116**, 6146–6151 (2019).

18. S. Felkai, *et al.*, CLK-1 controls respiration, behavior and aging in the nematode Caenorhabditis elegans. *EMBO J.* **18**, 1783–1792 (1999).

19. C. Yee, W. Yang, S. Hekimi, The intrinsic apoptosis pathway mediates the pro-longevity response to mitochondrial ROS in C elegans. *Cell* **157**, 897–909 (2014).

20. B. Lakowski, S. Hekimi, The genetics of caloric restriction in Caenorhabditis elegans. *Proc. Natl. Acad. Sci. U. S. A.* **95**, 13091–13096 (1998).

21. B. N. Heestand, *et al.*, Dietary Restriction Induced Longevity Is Mediated by Nuclear Receptor NHR-62 in Caenorhabditis elegans. *PLoS Genet.* **9** (2013).

22. A. Salminen, K. Kaarniranta, AMP-activated protein kinase (AMPK) controls the aging process via an integrated signaling network. *Ageing Res. Rev.* **11**, 230–241 (2012).

23. K. Burkewitz, Y. Zhang, W. B. Mair, AMPK at the nexus of energetics and aging. *Cell Metab.* **20**, 10–25 (2014).

24. H. J. Weir, *et al.*, Dietary Restriction and AMPK Increase Lifespan via Mitochondrial Network and Peroxisome Remodeling. *Cell Metab.* **26**, 884-896.e5 (2017).

25. W. Mair, *et al.*, Lifespan extension induced by AMPK and calcineurin is mediated by CRTC-1 and CREB. *Nature* **470**, 404–408 (2011).

26. D. Chen, *et al.*, Germline Signaling Mediates the Synergistically Prolonged Longevity Produced by Double Mutations in daf-2 and rsks-1 in C.elegans. *Cell Rep.* **5**, 1600–1610 (2013).

27. S. Herzig, R. J. Shaw, AMPK: Guardian of metabolism and mitochondrial homeostasis. *Nat. Rev. Mol. Cell Biol.* **19**, 121–135 (2018).

28. C. J. Fiorese, *et al.*, The Transcription Factor ATF5 Mediates a Mammalian Mitochondrial UPR. *Curr. Biol.* **26**, 2037–2043 (2016).

29. Q. Jiang, *et al.*, S6K1-mediated phosphorylation of PDK1 impairs AKT kinase activity and oncogenic functions. *Nat. Commun.* **13**, 1–14 (2022).

30. J. Durieux, S. Wolff, A. Dillin, The cell-non-autonomous nature of electron transport chain-mediated longevity. *Cell* **144**, 79–91 (2011).

31. D. A. Allen, M. M. Yaqoob, S. M. Harwood, Mechanisms of high glucose-induced apoptosis and its relationship to diabetic complications. *J. Nutr. Biochem.* **16**, 705–713 (2005).

32. R. P. Robertson, J. Harmon, P. O. Tran, Y. Tanaka, H. Takahashi, Glucose Toxicity in _-Cells: Type 2 Diabetes, Good Radicals Gone Bad, and the Glutathione Connection. *Diabetes* **52**, 581–587 (2003).

33. T. J. Schulz, *et al.*, Glucose Restriction Extends Caenorhabditis elegans Life Span by Inducing Mitochondrial Respiration and Increasing Oxidative Stress. *Cell Metab.* **6**, 280–293 (2007).

34. C. Cantó, J. Auwerx, Calorie restriction: Is AMPK a key sensor and effector? *Physiology*

26, 214–224 (2011).

35. I. R. Lanza, *et al.*, Chronic caloric restriction preserves mitochondrial function in senescence without increasing mitochondrial biogenesis. *Cell Metab.* **16**, 777–788 (2012).

36. X. Wang, X. J. Chen, A cytosolic network suppressing mitochondria-mediated proteostatic stress and cell death. *Nature* **524**, 481–484 (2015).

37. C. M. Haynes, Surviving import failure. *Nature* **524**, 419–420 (2015).

38. L. Wrobel, *et al.*, Mistargeted mitochondrial proteins activate a proteostatic response in the cytosol. *Nature* **524**, 485–488 (2015).

39. Si. C. Johnson, *et al.*, mTOR Inhibition Alleviates Mitochondrial Disease in a Mouse Model of Leigh Syndrome. *Science (80-.).* **342**, 1524–1529 (2013).

Figures

Figure 1: Inhibition of NHR-2 and NHR-180 suppresses slow growth in *atfs-1* null mutants. A Schematic showing the RNAi screen in the *atfs-1(null)* worms to identify suppressors of growth delay. **B-C** *nhr-2*(RNAi) and *nhr-180*(RNAi) treatment leads to faster growth of *atfs-1(null)* animals. Bar graphs plotted as % of adults after 55 hrs from egg stage. N =3, biologically independent replicates. *p< 0.05 Error bars mean ± SD (one-way ANOVA). **D, E** Growth as % adults of *clk-1(qm30)* mutants and *isp-1(qm150)* mutants (**F, G**) after control, *nhr-2* or *nhr-180* RNAi from the egg stage. N =3, biologically independent replicates. *p< 0.05 Error bars mean ± SD (one-way ANOVA). **H** Representative images of TMRE stained wildtype, *atfs-1(null)* and *atfs-1(null); nhr-180*(RNAi). Scale bar, 10 µm. N =3, biologically independent replicates. Bar graph showing the mean TMRE intensity per area. N=15 animals, ***p < 0.0001 (one-way ANOVA). **I, J** Lifespan graphs of wildtype (N2), *atfs-1(null)* and *atfs-1(null); nhr-180*(RNAi) animals. N =3, biologically independent replicates. *p < 0.01 (log-rank test). **K** Quantification of mtDNA by qPCR in *atfs-1(null)* worms raised on control(RNAi) or *nhr-180*(RNAi). N = 3, biologically independent samples. **p < 0.01 (two-tailed Student's t-test).

Figure 2: Loss of NHR-180 leads to increased TMRE staining and mtDNA content. A Schematics showing the exons (boxes) and introns (lines) of NHR-180 protein with the conserved domains. *cmh19* CRISPR allele with multiple stop codons is shown in red. **b-c** Lifespan graphs for wildtype and *nhr-180* mutants at 20°C (**B**) and 25°C (**C**). **D** Lifespan graph for *atfs-1(null)* and *atfs-1(null); nhr-180(cmh19)* mutants at 20°C. N =3, biologically independent replicates. *p < 0.01 (**B, D**) n.s. (**C**) (log-rank test). **E** Representative images of TMRE stained wildtype, *nhr-180(cmh19), atfs-1(null)* and *atfs-1(null); nhr-180(cmh19)* at the young adult stage. Scale bar, 10 µm. N =3, biologically independent replicates. **F** Bar graph showing the mean TMRE intensity per area. N=15 animals per condition, ***p < 0.0001 (one-way ANOVA). **G** Quantification of mtDNA by qPCR in wildtype, *nhr-180(cmh19), atfs-1(null)* and *atfs-1(null); nhr-180(cmh19)*. N = 3, biologically independent samples. **p < 0.01 (one-way ANOVA). **H** Representative images of TMRE stained wildtype and *nhr-180(cmh19)* at day-4 of adult stage. Scale bar, 10 µm. N =3, biologically independent replicates. **I** Bar graphs showing total number of eggs laid by wildtype, *nhr-180(cmh19), atfs-1(null)* and *atfs-1(null); nhr-180(cmh19)*. N = 3, biologically independent samples. **p < 0.01, ***p < 0.001 (one-way ANOVA). **J** Graph showing % survivability of worms in 100mM paraquat concentration at different time points. N = 3, biologically independent samples. **p < 0.01 (one-way ANOVA). **K** Lifespan of wildtype and

nhr-180(cmh19) on *P. aeruginosa*. N =3, biologically independent replicates. $p > 0.05$ (n.s.) (log-rank test).

Figure 3: NHR-180 is expressed in the intestine, muscle, and hypodermis. A Schematic showing the plasmid construct of *nhr-180$_{pr}$::NHR-180-GFP* translational reporter. **B** Representative images of NHR-180-GFP strain in the intestinal cells, muscle cells, and hypodermal cells. Scale bar, 50 µm **C** Representative NHR-180-GFP images at the young adult stage after growing worms from the L4 stage on untreated *E. coli* plates (control), *E. coli* plates treated with paraquat, *P. aeruginosa* plates, and *E. coli* plates treated with tunicamycin. Scale bar, 100 µm. **D** Representative NHR-180-GFP images at the young adult stage after control(RNAi) and *nhr-180(*RNAi). Scale bar, 100 µm. **E** Quantification of *nhr-180* transcripts by qPCR in wildtype worms with and without paraquat treatment. N = 3, biologically independent samples. ***$p < 0.001$ (two-tailed Student's t-test). **F** Table showing the fold change in the *nhr-180* expression in different mitochondrial mutants.

Figure 4: Loss of NHR-180 reverses gene expression in *atfs-1(null)* and other OXPHOS mutants. A Heatmap showing gene expression changes in wildtype (N2), *nhr-180(null), atfs-1(null)* and *atfs-1(null); nhr-180(null)* mutants. **B** Graph showing significantly different expression of genes in nhr-180(cmh19) mutants versus wildtype (N2). **C** Bubble plot showing the normalized enrichment scores of gene ontology classes for differentially expressed genes in the *nhr-180* mutant. **D** Quantification of UPR^{mt} reporter *hsp-6* transcripts by qPCR in wildtype, and *nhr-180(cmh19)* at different larval stages. N = 3, biologically independent samples. ***$p < 0.001$ (one-way ANOVA). **E** Heatmap listing the genes in *atfs-1(null)* that are reversed in the double mutants of *atfs-1(null); nhr-180(cmh19).* **F** Venn diagram showing the common sets of genes between OXPHOS mutants and *nhr-180* mutants. (See supplementary Table 3 for a complete list of genes).

Figure 5: AAK-2 activation or starvation promotes mitochondrial recovery in *atfs-1* mutants. A Venn diagram showing the common sets of genes between *eat-2* mutant and *nhr-180* mutants. (See supplementary Table 4 for a complete list of genes). **B** Representative images of TMRE stained wildtype, CA-AAK-2, *rsks-1*(RNAi), *atfs-1(null)*, *atfs-1(null); CA-AAK-2* and *atfs-1(null); rsks-1*(RNAi) at the young adult stage. Scale bar, 10 µm. N =3, biologically independent replicates. **C** Bar graph showing the mean TMRE intensity per area. N=15 animals per condition, ***$p < 0.0001$ (one-way ANOVA). **D, E** Lifespan graphs of wildtype (N2), CA-AAK-

2, *rsks-1*(RNAi), *atfs-1(null)*, *atfs-1(null); CA-AAK-2* and *atfs-1(null); rsks-1*(RNAi) animals. N =3, biologically independent replicates. *$p < 0.01$ (log-rank test). **F** Quantification of mtDNA by qPCR in wildtype and *atfs-1(null)* following control(RNAi) or *rsks-1*(RNAi). N = 3, biologically independent samples. **$p < 0.01$ (one-way ANOVA). **G** Schematic showing the starvation steps followed for wildtype(N2) and *atfs-1(null)* worms that improved lifespan (**H**) and other phenotypes. **I** Quantification of mtDNA by qPCR in wildtype and ATF5(-) cells after treatment with S6 kinase inhibitor at different concentrations. N = 3, biologically independent samples. **$p < 0.01$ (one-way ANOVA

Table 1: List of mitochondrial genes downregulated in *nhr-180* mutants. Genes involved in mitochondrial translation are greyed.

Table 2: List of cytosolic translation machinery genes that are down in *nhr-180* mutants.

Supplementary Table 1: Differentially expressed genes in *nhr-180* mutants vs N2.

Supplementary Table 2: Genes that are upregulated in the *atfs-1(null); nhr-180(cmh19)* mutants compared to *atfs-1(null)*.

Supplementary Table 3: Common differentially expressed genes between *nhr-180* and OXPHOS mutants.

Supplementary Table 4: Common differentially expressed between *nhr-180* and *eat-2* mutants.

Supplementary Table 5: Common differentially expressed between *nhr-180* and *CA-AAK-2* mutants.

Figure 1: Inhibition of NHR-2 and NHR-180 suppresses slow growth in *atfs-1* null and OXPHOS mutants.

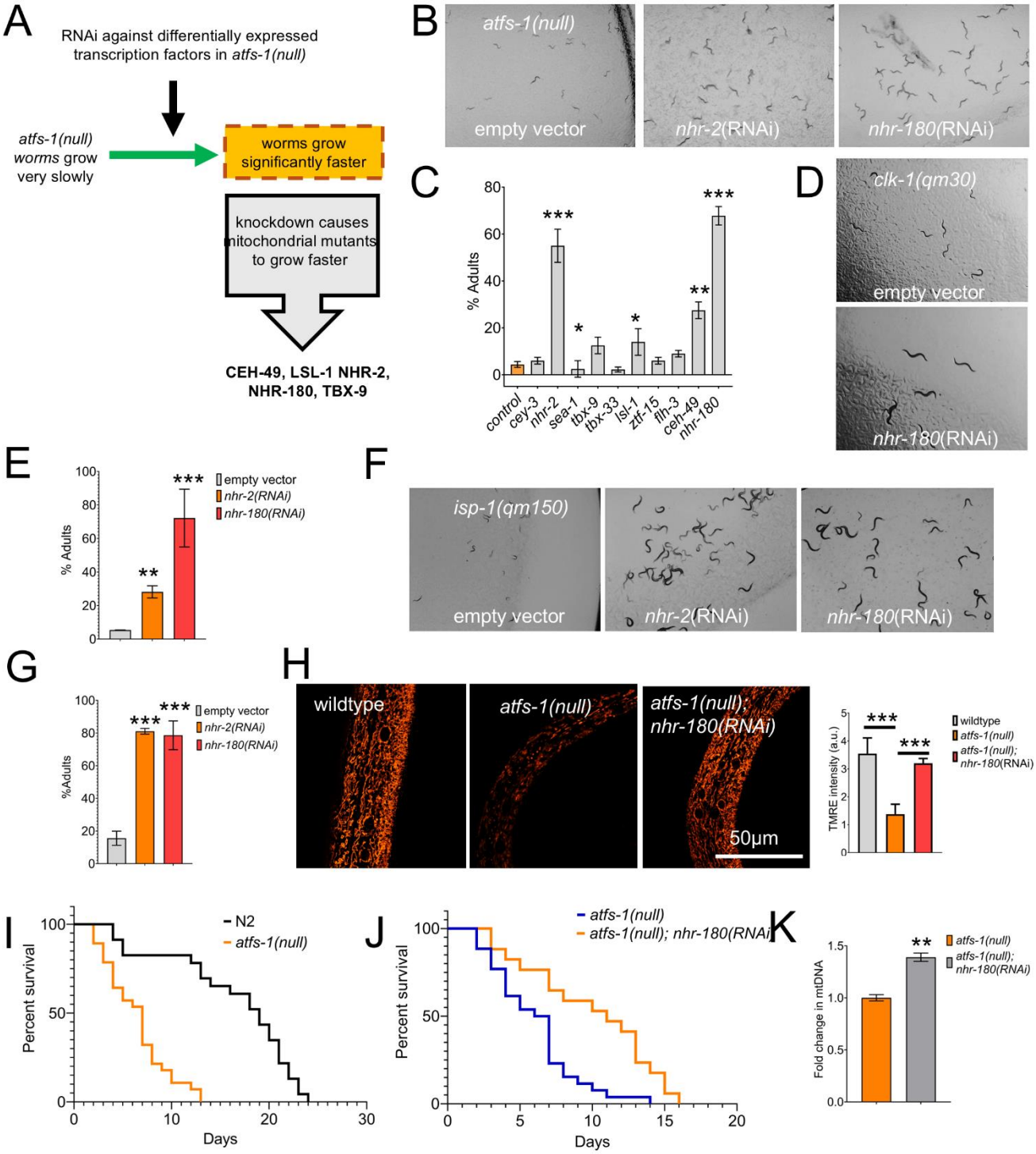

Figure 2: Loss of NHR-180 leads to increased TMRE staining and mtDNA content.

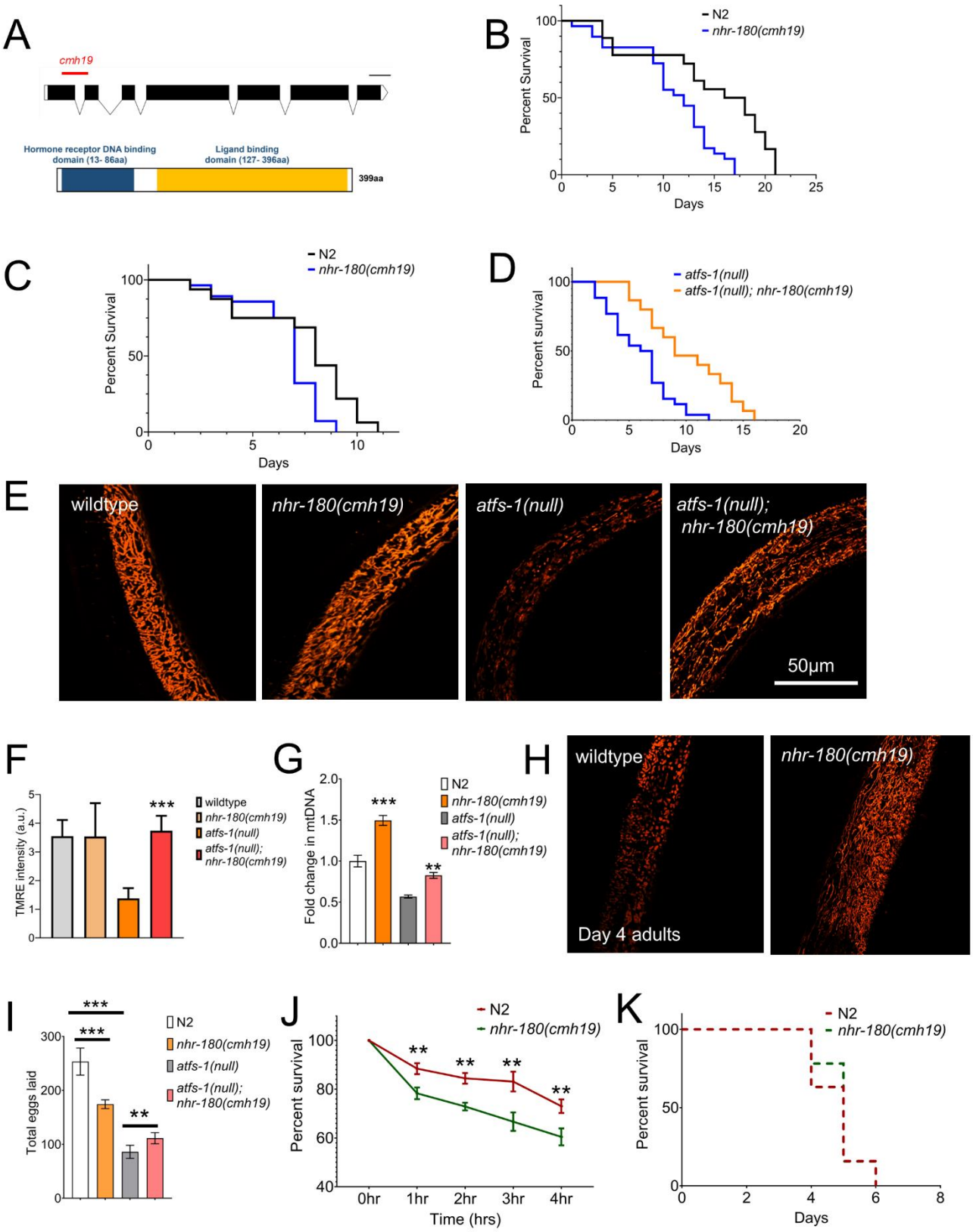

Figure 3: NHR-180 is expressed in the intestine, muscle, and hypodermis.

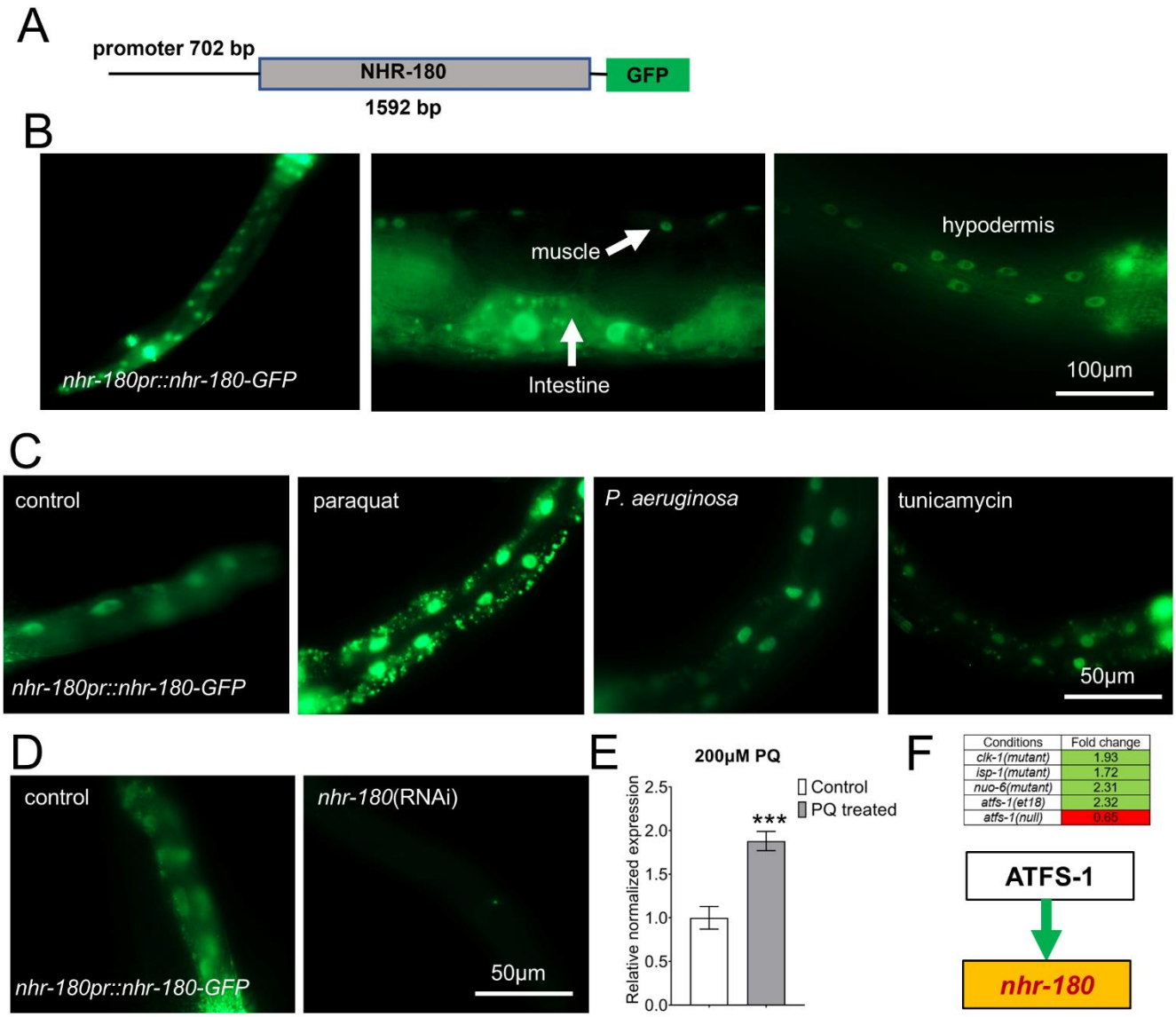

Figure 4: Loss of NHR-180 reverses gene expression in *atfs-1(null)* and other OXPHOS mutants.

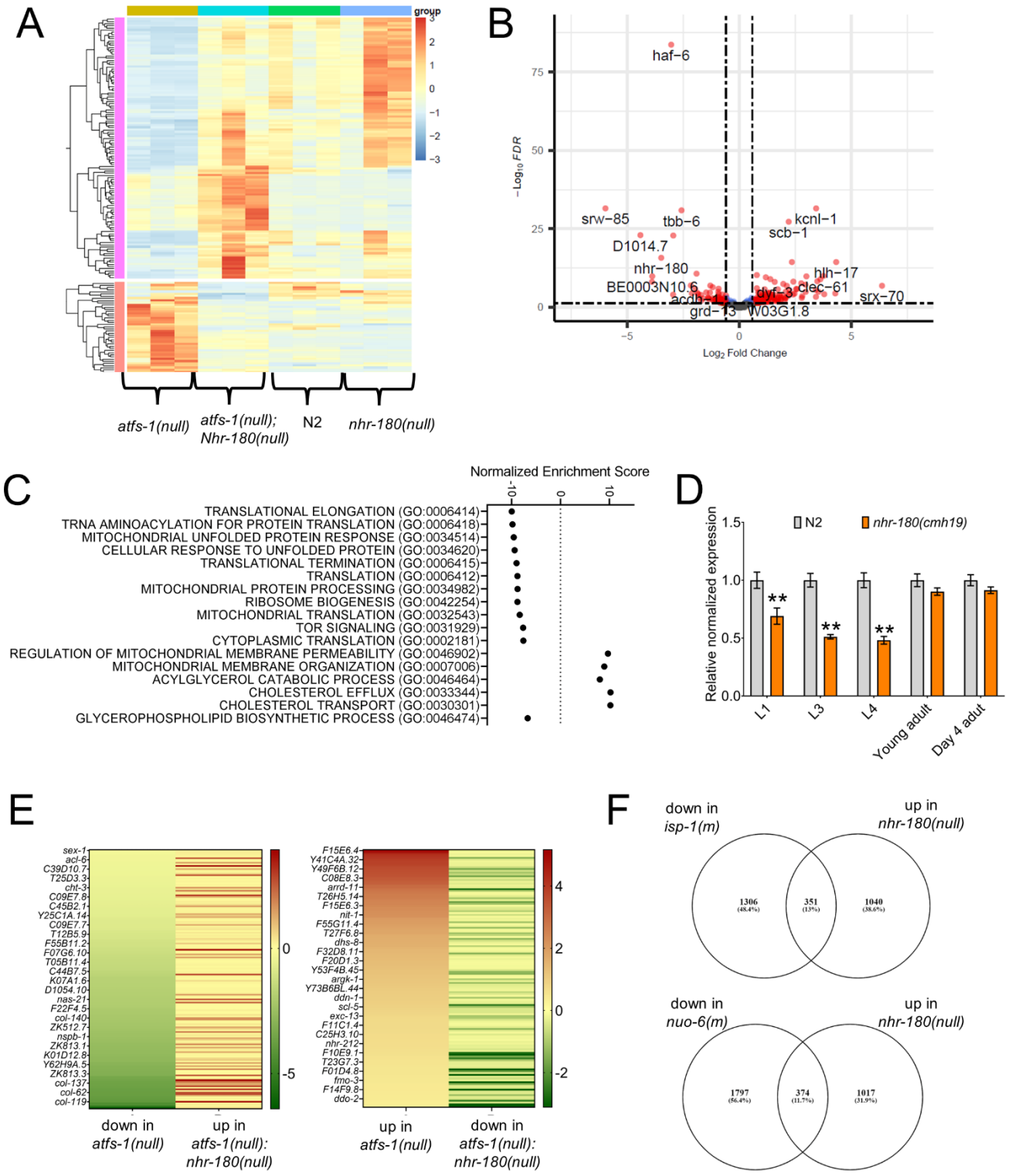

Figure 5: AAK-2 activation or starvation promotes mitochondrial recovery in *atfs-1* mutants.

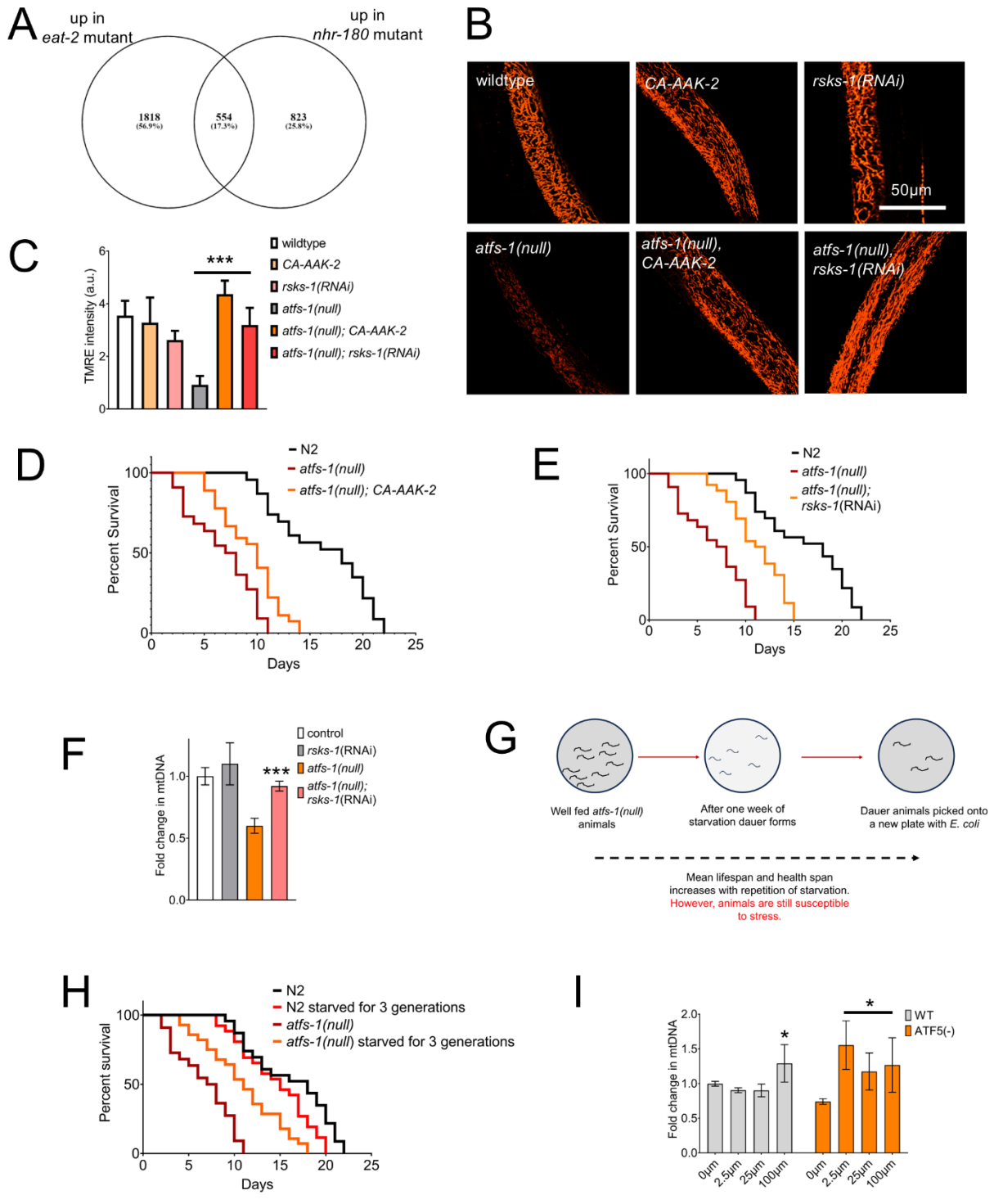

Table 1: List of mitochondrial genes downregulated in *nhr-180* mutants. Genes involved in mitochondrial translation are greyed.

Gene	Function in mitochondria
clu-1	Mitochondrial RNA binding activity
coq-8	predicted to have ATP binding activity and transferase activity\; is involved in ubiquinone biosynthetic process
drp-1	is involved in apoptotic mitochondrial changes, embryo development, and mitochondrial fission
hars-1	ortholog of human HARS (histidyl-tRNA synthetase) and HARS2 (histidyl-tRNA synthetase 2, mitochondrial)
hsp-6	Mitochondrial chaperone
phb-1	Mitochondrial metabolism
phb-2	Mitochondrial metabolism
glp-4	ortholog of human VARS (valyl-tRNA synthetase) and VARS2 (valyl-tRNA synthetase 2, mitochondrial
tufm-1	translation elongation factor activity
tufm-2	translation elongation factor activity
tomm-40	is involved in protein import into the mitochondrial matrix
mrps-31	ortholog of human MRPS31 (mitochondrial ribosomal protein S31)
c34c12.8	ortholog of human GRPEL1 (GrpE like 1, mitochondrial) and GRPEL2\; is predicted to have adenyl-nucleotide exchange factor activity
timm-23	is involved in protein import into the mitochondrial matrix
gfm-1	predicted to have GTPase activity and translation elongation factor activity
idhg-1	predicted to have NAD binding activity, isocitrate dehydrogenase (NAD+) activity
atad-3	ortholog of human ATAD3A (ATPase family, AAA domain containing 3A) and ATAD3B (ATPase family, AAA domain containing 3B)
tsfm-1	have translation elongation factor activity

idh-1	predicted to have isocitrate dehydrogenase (NADP+) activity and metal ion binding activity
k11h3.3	Mitochondrial substrate/solute carrier
r07e3.4	ortholog of human SLC25A4 (solute carrier family 25 member 4), SLC25A5 (solute carrier family 25 member 5), and SLC25A6 (solute carrier family 25 member 6)
cox-15	ortholog of human COX15 (cytochrome c oxidase assembly homolog COX15)
cchl-1	have holocytochrome-c synthase activity and metal ion binding activity
hphd-1	ortholog of human ADHFE1 (alcohol dehydrogenase, iron-containing 1)\; is predicted to have hydroxyacid-oxoacid transhydrogenase activity
mrps-35	ortholog of human MRPS35 (mitochondrial ribosomal protein S35)
lonp-1	involved in the protein catabolic process
c35d10.5	human UQCC1 (ubiquinol-cytochrome c reductase complex assembly factor 1)
sucg-1	nucleoside phosphate binding activity, and succinate-CoA ligase (GDP-forming) activity
timm-17b.1	have P-P-bond-hydrolysis-driven protein transmembrane transporter activity
mrpl-1	human MRPL1 (mitochondrial ribosomal protein L1)
tin-44	ortholog of human TIMM44 (translocase of inner mitochondrial membrane 44)
y22d7al.10	human HSPE1 exhibits chaperone binding activity
mrpl-17	a structural constituent of ribosome
mrpl-45	human MRPL45 (mitochondrial ribosomal protein L45)
tomm-70	Mitochondrial transmembrane translocase
mrpl-42	Mitochondrial ribosomal protein
c24g6.13	encode a protein with the following domain: Cytochrome c oxidase assembly protein COX16

Table 2: List of cytosolic translation machinery genes that are downregulated in *nhr-180* mutants.

Gene	Function
eftu-2	ortholog of human EFTUD2 (elongation factor Tu GTP binding domain containing 2)
eef-2	translation elongation factor activity
eif-3.c	have translation initiation factor activity and translation initiation factor binding activity
eif-3.d	have translation initiation factor activity and translation initiation factor binding activity
eif-3.e	have translation initiation factor activity and translation initiation factor binding activity
eif-3.h	have translation initiation factor activity and translation initiation factor binding activity
fars-3	ortholog of human FARSB (phenylalanyl-tRNA synthetase subunit beta)
eif-2a	ortholog of human EIF2A (eukaryotic translation initiation factor 2A)
eif-3.l	ortholog of human EIF3L (eukaryotic translation initiation factor 3 subunit L)
cif-1	ortholog of human EIF3M (eukaryotic translation initiation factor 3 subunit M)
erfa-1	have translation release factor activity
y73b3a.18	ortholog of human RPL7A (ribosomal protein L7a)